

# Emergence of two types of terrestrial planet on solidification of magma ocean

Keiko Hamano<sup>1</sup>, Yutaka Abe<sup>1</sup> & Hidenori Genda<sup>1,2</sup>

Understanding the origins of the diversity in terrestrial planets is a fundamental goal in Earth and planetary sciences. In the Solar System, Venus has a similar size and bulk composition to those of Earth, but it lacks water<sup>1–3</sup>. Because a richer variety of exoplanets is expected to be discovered, prediction of their atmospheres and surface environments requires a general framework for planetary evolution. Here we show that terrestrial planets can be divided into two distinct types on the basis of their evolutionary history during solidification from the initially hot molten state expected from the standard formation model<sup>4,5</sup>. Even if, apart from their orbits, they were identical just after formation, the solidified planets can have different characteristics. A type I planet, which is formed beyond a certain critical distance from the host star, solidifies within several million years. If the planet acquires water during formation, most of this water is retained and forms the earliest oceans. In contrast, on a type II planet, which is formed inside the critical distance, a magma ocean can be sustained for longer, even with a larger initial amount of water. Its duration could be as long as 100 million years if the planet is formed together with a mass of water comparable to the total inventory of the modern Earth. Hydrodynamic escape desiccates type II planets during the slow solidification process. Although Earth is categorized as type I, it is not clear which type Venus is because its orbital distance is close to the critical distance. However, because the dryness of the surface and mantle predicted for type II planets is consistent with the characteristics of Venus, it may be representative of type II planets. Also, future observations may have a chance to detect not only terrestrial exoplanets covered with water ocean but also those covered with magma ocean around a young star.

Theoretical studies on planet formation suggest that Earth-sized planets (Earth and Venus) should form as a result of giant impacts between protoplanets<sup>4</sup>, and probably all start their lives in a globally molten state<sup>5</sup>. The earliest phase of planetary evolution is thus solidification of a magma ocean, which provides the initial conditions for mantle differentiation and distribution of volatiles between the interior and the surface<sup>6</sup>. The timing of the end of this phase also determines the starting point for subsequent events such as water ocean formation, and possibly the onset of plate tectonics and the development of life.

The thermal evolution of a magma ocean is closely linked to the formation of a steam atmosphere<sup>6–8</sup>. A massive steam atmosphere decreases outgoing radiation from the planet through its strong greenhouse effects, and thus delays the solidification process. Degassing from a solidifying magma ocean can in turn greatly increase the amount of the steam atmosphere<sup>6</sup>. Therefore, evaluating the outgoing radiation during atmospheric evolution is the key to understanding the earliest thermal history of the planet.

Particularly for a hot steam atmosphere above a magma ocean, previous studies have shown that the outgoing radiation has a lower limit (about  $300 \text{ W m}^{-2}$ ) owing to saturation of the upper troposphere with water vapour<sup>9–11</sup>. This is because its thermal structure is uniquely determined by the saturated-vapour-pressure curve of water (see

ref. 11 for a further explanation). Because the net incoming stellar radiation in the zone of formation of terrestrial planets can be smaller or larger than this radiation limit, it can be speculated from heat balance that the presence of such a limit would produce an evolutionary dichotomy between terrestrial planets. The effect of the radiation limit, however, was neglected in a previously proposed coupled model for a deep magma ocean and steam atmosphere<sup>6</sup>. In addition, the greenhouse effect of water vapour has not been fully considered.

Here we perform radiative–convective equilibrium calculations to enable our model to be used to calculate the radiation limit for a saturated steam atmosphere. In addition we take into account the water loss associated with hydrodynamic escape<sup>12</sup>, which is expected to occur in parallel with magma-ocean solidification. Competition between degassing and water loss determines whether the steam atmosphere grows or escapes. This would affect not only the thermal evolution of planets but also the planetary water inventory at the time of complete solidification.

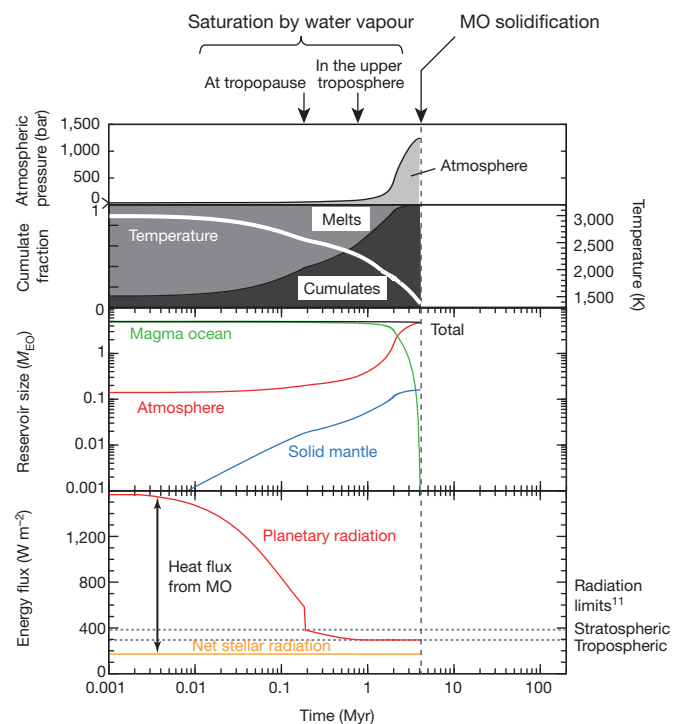


**Figure 1 | Typical evolution of a type I planet.** Evolution of a planet located at 1 AU, with an initial water mass of five times the current ocean mass on Earth ( $M_{\text{EO}}$ ,  $1.4 \times 10^{21} \text{ kg}$ ). The grey dotted lines in the bottom panel indicate the radiation limits<sup>11</sup>. At  $\sim 0.7 \text{ Myr}$ , the planetary radiation reaches the tropospheric radiation limit. After that, the heat flux from the magma ocean (MO) becomes constant. This results in rapid solidification at  $\sim 4 \text{ Myr}$ . The solidification time and final water partitioning are comparable to those reported in ref. 6 for a MO 2,000 km deep on Earth and a total water mass of  $\sim 10M_{\text{EO}}$ .

<sup>1</sup>Department of Earth and Planetary Science, The University of Tokyo, 7-3-1 Hongo, Bunkyo-ku, Tokyo 113-0033, Japan. <sup>2</sup>Earth-Life Science Institute, Tokyo Institute of Technology, 2-12-1 Ookayama, Meguro-ku, Tokyo 152-8551, Japan.

Figure 1 shows the typical evolution of an Earth-sized planet located at a distance of 1 AU from its parent star. Because of the high solubility of water in silicate melts, a sizeable fraction of the water dissolves in the initial deep magma ocean. As the magma solidifies, degassing of water from the interior leads to an increase in the atmospheric mass. At about 0.2 million years (Myr), because of the growth of the atmosphere combined with the decrease in temperature, the atmosphere starts to be saturated with water vapour at the tropopause. As the saturation front moves deeper into the troposphere, the planetary radiation decreases until it finally becomes equal to the tropospheric radiation limit at about 0.7 Myr. The outgoing radiation flux then remains constant throughout the subsequent solidification period.

The overall solidification time is about 4 Myr in this case, and is mainly determined by the minimum net heat flux; this is defined as the difference between the radiation limit and the net incident stellar radiation. The existence of a minimum heat flux after saturation gives rise to rapid solidification because further atmospheric growth has no effect on the cooling rate of the planet. Hydrodynamic escape makes little contribution to the water inventory during the short magma-ocean period. We refer to this type of planet as type I.

This mechanism does not apply to the evolution of a planet at 0.7 AU (Fig. 2), in which the net incident stellar radiation exceeds the tropospheric radiation limit. In the earlier stages up to  $\sim 0.2$  Myr, its evolution is similar to that of a type I planet. However, at  $\sim 1$  Myr the outgoing radiation almost balances the net incident stellar radiation before a sufficiently deep part of the troposphere becomes saturated. This results in an extremely low heat flux so that the magma ocean is sustained for about 100 Myr, much longer than the value of 4 Myr at 1 AU, for an initial water amount of five times the current ocean mass on Earth ( $5M_{\text{EO}}$ ). During this period there is a large decrease in the total water inventory of the planet.

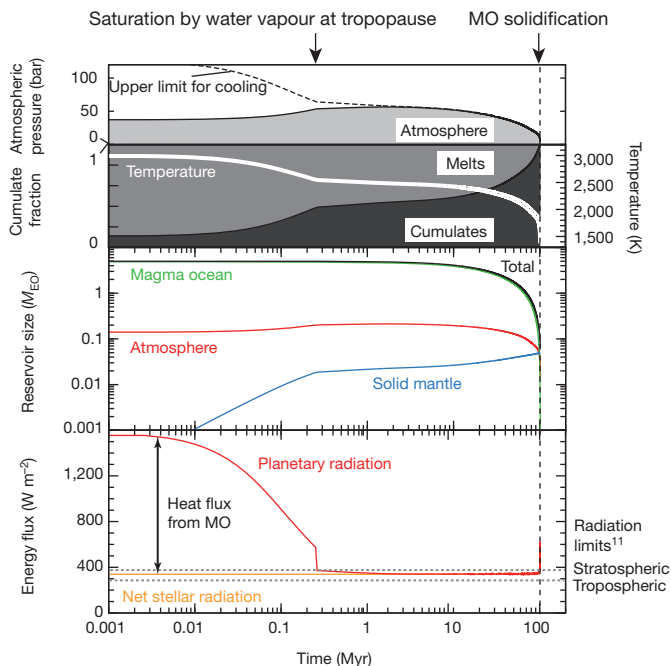
The solidification rate is mainly governed by the water loss rate due to hydrodynamic escape. Because the outgoing radiation must exceed

the incident stellar radiation for cooling, the steam atmosphere must be optically thinner for lower surface temperatures (Fig. 2), so that a net loss of the steam atmosphere is required. We refer to this type of planet as type II.

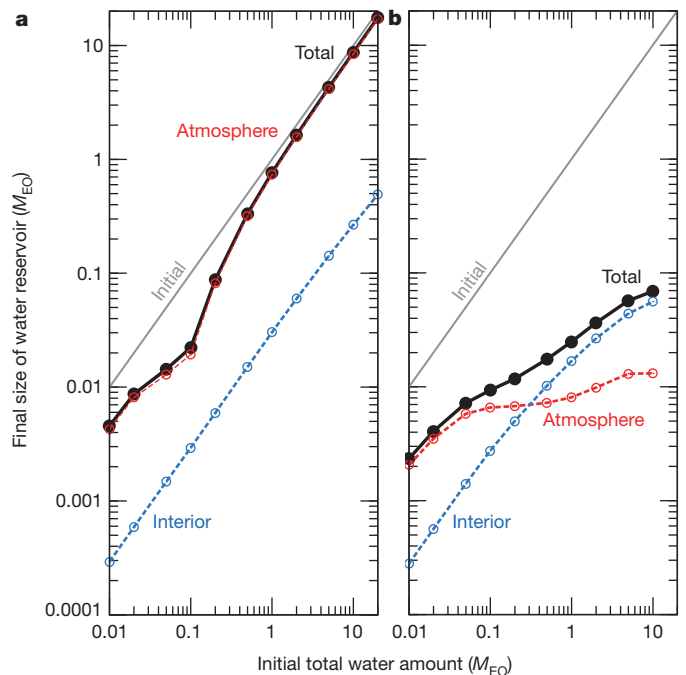
These two types of planet also have a different partitioning of water between the atmosphere and the interior (Fig. 3). For the type I planet at 1 AU, the total water inventory becomes less susceptible to loss for larger initial water masses. The primary water reservoir is the steam atmosphere, whereas the deep interior accounts for only a small percentage of the planetary water inventory. In contrast, the type II planet at 0.7 AU becomes desiccated during the longer magma-ocean period. The final total water inventory is less than  $0.1M_{\text{EO}}$  even for an initial value of  $10M_{\text{EO}}$ . In addition, as the initial water inventory increases, the interior reservoir becomes larger than that of the atmosphere.

Figure 4 shows the solidification time and final total water inventory for Earth-sized planets within the terrestrial planet formation zone. The solidification time (see Supplementary Information for analytical expressions) is seen to peak at about 0.8 AU. Planets located beyond this range are classified as type I, whereas those inside it are classified as type II. Type I planets have maximum solidification times typically as short as several million years owing to the minimum heat flux. Because only a limited amount of hydrodynamic escape can occur within such a short period, it has a reduced impact on the thermal history and water budget of the planet. Soon after solidification, water oceans would probably form on the surface.

For a type I planet, the initial total water inventory simply affects the volume of the earliest oceans, whereas it has a strong influence on the solidification time for a type II planet. As seen in Fig. 4, the duration of the magma-ocean phase agrees well with the time required for total loss of the primordial water. This reflects the fact that the type II planet must lose water to cool down, and consequently a larger water endowment results in a longer magma-ocean period. The final total water inventory of type II planets never exceeds  $0.1 M_{\text{EO}}$ , irrespective of the initial value.



**Figure 2 | Typical evolution of a type II planet.** As in Fig. 1, but for an orbital distance of 0.7 AU. The net incident stellar radiation is larger than the tropospheric radiation limit. At  $\sim 1$  Myr, planetary radiation almost balances the net stellar radiation. The subsequent heat flux from the MO is controlled by the rate of water loss. The dashed black line in the top panel represents the upper limit of atmospheric pressure for cooling, for which the planetary radiation is equal to the net stellar flux. The MO period is  $\sim 100$  Myr, much longer than that for a type I planet.



**Figure 3 | Water partitioning between steam atmosphere and planetary interior.** The amount of water depends on the rate of loss and the duration of the MO period. **a**, Planet at 1 AU (type I). Most of the primordial water remains and contributes to the steam atmosphere at the time of complete solidification. **b**, Planet at 0.7 AU (type II). The final total mass of water is less than  $0.1M_{\text{EO}}$ . The planetary interior may become the dominant reservoir if water is incorporated before the silicate melts become desiccated. The effect of a surface thermal boundary layer is discussed in Supplementary Information.

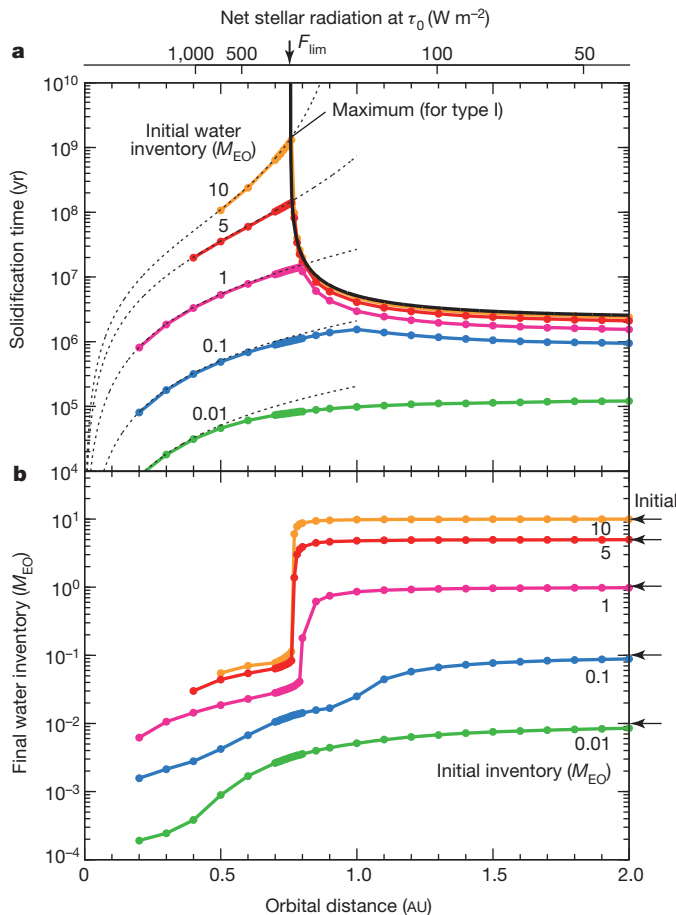


**Figure 4 | Two distinct types of terrestrial planet.** The upper x axis shows the corresponding initial net stellar radiation. The arrow indicates the tropospheric radiation limit. The critical orbital distance  $a_{\text{cr}}$  of  $\sim 0.76$  AU separates the orbital regimes of the two types of planet. **a**, Solidification time. The dotted lines show the time required for complete loss of primordial water. This provides a good approximation of the solidification time of type II planets. The maximum solidification time for type I planets is also shown (see Supplementary Information). **b**, Total water inventory at the time of complete solidification. A strong transition is exhibited at about  $a_{\text{cr}}$ .

The different mechanisms determining the solidification rate thus also lead to a sharp transition in the planetary water budget.

Whether a type I or a type II planet is formed around a star depends on the critical orbital distance  $a_{\text{cr}}$ , which is defined as the distance at which the net stellar flux that the planet receives equals the tropospheric radiation limit  $F_{\text{lim}}$  of the steam atmosphere,

$$a_{\text{cr}} \approx 0.76 \left( \frac{F_{\text{lim}}}{294 \text{ W m}^{-2}} \right)^{-1/2} \left( \frac{S_{\text{stl}}(\tau_0)}{0.7 S_{\odot}} \right)^{1/2} \left( \frac{1-\alpha}{1-0.3} \right)^{1/2} \text{ AU} \quad (1)$$

where  $S_{\text{stl}}(\tau_0)$  is the stellar constant at a stellar age  $\tau_0$  when solidification starts.  $S_{\odot}$  is the current solar constant and  $\alpha$  is the planetary albedo.  $a_{\text{cr}}$ , which is about 0.76 in our model, can range from about 0.6 to 0.8 AU, as a result of parameter uncertainties and the atmospheric model used.

Earth is located at a distance of 1 AU from the Sun, which is sufficiently far for it to be a type I planet. Its deep interior would probably have solidified within about 5 Myr, even if it had acquired as much or more water than the current total inventory ( $\sim 1.25\text{--}5M_{\text{EO}}$ )<sup>13</sup>. This would support the rapid solidification and ocean formation condition suggested from geochemical data<sup>14,15</sup>. The overall water budget would have been only slightly affected by hydrodynamic escape, but this modest loss might still have contributed to oxidization of the interior through selective escape of hydrogen over oxygen. If a simple assumption is made

that all of the dissociated oxygen atoms were consumed by oxidation of ferrous iron, the bulk  $\text{Fe}_2\text{O}_3$  content in the early mantle would have increased by up to about 0.07wt% during the first several million years of Earth's history. This value is comparable to the current  $\text{Fe}_2\text{O}_3$  content in the upper mantle ( $>0.2\text{wt}\%$ )<sup>16</sup> and is consistent with the idea of an oxidized mantle possibly as early as 4.4 Gyr ago (ref. 17).

Because Venus's orbital distance of about 0.72 AU places it on the border zone, it is not exactly clear which planetary type it should be classified as. However, the significant water loss for a type II planet during the magma-ocean period might explain its dry interior and the fate of the remnant oxygen. The absence of water on its surface<sup>1</sup> and interior<sup>2,3</sup> is conventionally explained in terms of an inherently dry origin<sup>18</sup> or hydrodynamic escape after ocean evaporation<sup>19</sup>. The latter situation corresponds to the case in which Venus is a type I planet in our classification. In this case, the dryness of its interior depends on degassing efficiency during the subsequent evolution. Alternatively, if Venus belongs to type II, the occurrence of planetary desiccation during solidification can explain the dryness of its current mantle<sup>2,3</sup>, even if it accreted with a certain amount of water. The presence of a dry mantle during the earliest stages might also have led to a subsequent tectonic evolution different from that of Earth<sup>20,21</sup> and possibly to the absence of a magnetic field<sup>22</sup>.

One problem associated with the hydrodynamic escape of water is the accumulation of dissociated oxygen in the atmosphere as a result of the preferential escape of hydrogen<sup>23</sup>, which would possibly lead to a shutdown of the hydrogen escape process itself. However, if Venus belongs to type II, the remnant oxygen issue can be avoided, regardless of the initial amount of water, because the abundant surface magma can act as a massive oxygen sink. Although the effects of other gaseous species such as carbon dioxide will need to be addressed in future work, the slight difference in the orbital distances of Earth and Venus might have been the critical factor making these planets totally different after solidification.

Although we have so far discussed only Earth-sized planets orbiting a Sun-like star, the conclusions can be qualitatively extended to all terrestrial planets that experienced global melting through giant impact. More than 750 exoplanets have already been confirmed<sup>24</sup>, and 2,300 candidates<sup>25</sup> have been identified. Future space missions such as the Terrestrial Planet Finder and Darwin will provide us with a catalogue of atmospheres and surface environments for terrestrial planets of various ages. The present results indicate that for habitable planets, rapid ocean formation would have occurred within several million years of planet formation. In addition, the prediction that type II planets undergo a long-lived ( $\sim 100$  Myr) magma-ocean stage suggests that, apart from permanently molten planets very close to the host star, there may be a chance of detecting still-molten terrestrial planets as a consequence of planetary formation, especially around young stars. Although the molten surface would be hard to detect through the thick atmosphere, it can in principle be identified by detecting gaseous species such as NaOH and KOH that are indicative of hot atmospheres<sup>26</sup>.

## METHODS SUMMARY

**Water reservoirs and budgets.** Partition of water between planetary reservoirs was treated in basically the same way as in ref. 6. We used water solubility in basaltic-composition melts calculated from a solubility model in ref. 27. Water partition coefficient into cumulates and mass fraction of interstitially trapped melts were fixed at  $10^{-4}$  and 0.01, respectively.

The water-loss rate was calculated from energy-limited escape rate of hydrogen<sup>12</sup> with a heating efficiency of 0.1 by assuming that all the dissociated oxygen would have been absorbed into the magma ocean. For the effects of the higher heating efficiency, see the online-only Methods and Supplementary Information section 4. We adopted an observational compilation of Sun-like stars for time-dependent extreme ultraviolet radiation<sup>28</sup>.

**Thermal evolution model.** Assuming that the atmosphere has a negligible heat capacity, the thermal evolution model was formulated on the basis of heat balance:

$$C_{p,pl}(T_m) \frac{dT_m}{dt} = -4\pi R^2 (F_{pl} - F_{stl}) \quad (2)$$

where  $C_{p,pl}(T_m)$  is the heat capacity of the planet at potential temperature  $T_m$  of the interior, and  $R$  is the planetary radius.  $F_{pl}$  and  $F_{stl}$  are the outgoing planetary radiation and the incoming net stellar radiation, respectively. Calculation starts from temperature of 3,000 K, which corresponds to a mostly molten state of the mantle, and stops when it reaches the solidus temperature at the surface (~1,370 K). We assumed that the whole silicate portion could transfer heat by convection and therefore contribute to the heat capacity. We obtained the heat capacity, including latent heat of fusion, as a function of potential temperature, from its adiabatic temperature profile calculated according to ref. 29.

The planetary radiation was calculated with a modified radiative–convective equilibrium model of grey atmosphere<sup>11</sup>. We also performed non-grey calculations (Supplementary Information). We adopted a solar standard model for luminosity enhancement with stellar age<sup>30</sup>. A planetary albedo of 0.3 was assumed for the net stellar radiation.

**Full Methods** and any associated references are available in the online version of the paper.

**Received 7 October 2012; accepted 5 April 2013.**

- Lewis, J. S. & Grinspoon, D. H. Vertical distribution of water in the atmosphere of Venus: a simple thermochemical explanation. *Science* **249**, 1273–1275 (1990).
- Nimmo, F. & McKenzie, D. Volcanism and tectonics on Venus. *Annu. Rev. Earth Planet. Sci.* **26**, 23–51 (1998).
- Kiefer, W. S., Richards, M. A., Hager, B. H. & Bills, B. G. A dynamic model of Venus's gravity field. *Geophys. Res. Lett.* **13**, 14–17 (1986).
- Chambers, J. E. & Wetherill, G. W. Making the terrestrial planets: *N*-body integrations of planetary embryos in three dimensions. *Icarus* **136**, 304–327 (1998).
- Canup, R. M. Dynamics of lunar formation. *Annu. Rev. Astron. Astrophys.* **42**, 441–475 (2004).
- Elkins-Tanton, L. T. Linked magma ocean solidification and atmospheric growth for Earth and Mars. *Earth Planet. Sci. Lett.* **271**, 181–191 (2008).
- Matsui, T. & Abe, Y. Evolution of an impact-induced atmosphere and magma ocean on the accreting Earth. *Nature* **319**, 303–305 (1986).
- Zahnle, K. J., Kasting, J. F. & Pollack, J. B. Evolution of a steam atmosphere during Earth's accretion. *Icarus* **74**, 62–97 (1988).
- Abe, Y. & Matsui, T. Evolution of an impact-generated H<sub>2</sub>O–CO<sub>2</sub> atmosphere and formation of a hot proto-ocean on Earth. *J. Atmos. Sci.* **45**, 3081–3101 (1988).
- Kasting, J. F. Runaway and moist greenhouse atmospheres and the evolution of Earth and Venus. *Icarus* **74**, 472–494 (1988).
- Nakajima, S., Hayashi, Y. & Abe, Y. A study on the 'runaway greenhouse effect' with a one-dimensional radiative–convective equilibrium model. *J. Atmos. Sci.* **49**, 2256–2266 (1992).
- Watson, A. J., Donahue, T. M. & Walker, J. C. G. The dynamics of a rapidly escaping atmosphere: applications to the evolution of Earth and Venus. *Icarus* **48**, 150–166 (1981).
- Hirschmann, M. M. Water, melting, and the deep Earth H<sub>2</sub>O cycle. *Annu. Rev. Earth Planet. Sci.* **34**, 629–653 (2006).
- Caro, G. Early silicate Earth differentiation. *Annu. Rev. Earth Planet. Sci.* **39**, 31–58 (2011).

- Cavosie, A. J., Valley, J. W., Wilde, S. A. & Edinburgh Ion Microprobe Facility. Magmatic  $\delta^{18}\text{O}$  in 4400–3900 Ma detrital zircons: a record of the alteration and recycling of crust in the Early Archean. *Earth Planet. Sci. Lett.* **235**, 663–681 (2005).
- Canil, D. & O'Neill, H. St C. Distribution of ferric iron in some upper-mantle assemblages. *J. Petrol.* **37**, 609–635 (1996).
- Trail, D., Watson, E. B. & Tailby, N. D. The oxidation state of Hadean magmas and implications for early Earth's atmosphere. *Nature* **480**, 79–82 (2011).
- Lewis, J. S. Venus: atmospheric and lithospheric composition. *Earth Planet. Sci. Lett.* **10**, 73–80 (1970).
- Kasting, J. F. & Pollack, J. B. Loss of water from Venus. I. Hydrodynamic escape of hydrogen. *Icarus* **53**, 479–508 (1983).
- Mackwell, S. J., Zimmerman, M. E. & Kohlstedt, D. L. High-temperature deformation of dry diabase with applications to tectonics on Venus. *J. Geophys. Res.* **103**, 975–984 (1998).
- Moresi, L. & Solomatov, V. Mantle convection with a brittle lithosphere: thoughts on the global tectonic styles of the Earth and Venus. *Geophys. J. Int.* **133**, 669–682 (1998).
- Nimmo, F. Why does Venus lack a magnetic field? *Geology* **30**, 987–990 (2002).
- Chassefière, E. Hydrodynamic escape of oxygen from primitive atmospheres: applications to the cases of Venus and Mars. *Icarus* **124**, 537–552 (1996).
- The Extrasolar Planets Encyclopedia. <<http://exoplanet.eu/>> (2012).
- Batalha, N. M. *et al.* Planetary candidates observed by *Kepler*. III. Analysis of the first 16 months of data. *Astrophys. J. Suppl. S.* **204**, 24, <http://dx.doi.org/10.1088/0067-0049/204/2/24> (2013).
- Schaefer, L., Lodders, K. & Fegley B. Vaporization of the Earth: application to exoplanet atmospheres. *Astrophys. J.* **755**, 41, <http://dx.doi.org/10.1088/0004-637X/755/1/41> (2012).
- Papale, P. Modeling of the solubility of a one-component H<sub>2</sub>O or CO<sub>2</sub> fluid in silicate liquids. *Contrib. Mineral. Petrol.* **126**, 237–251 (1997).
- Ribas, I., Guinan, E. F., Güdel, M. & Audard, M. Evolution of the solar activity over time and effects on planetary atmospheres. I. High-energy irradiances (1–1700 Å). *Astrophys. J.* **622**, 680–694 (2005).
- Abe, Y. Thermal and chemical evolution of the terrestrial magma ocean. *Phys. Earth Planet. Inter.* **100**, 27–39 (1997).
- Gough, D. O. Solar interior structure and luminosity variations. *Sol. Phys.* **74**, 21–34 (1981).

**Supplementary Information** is available in the online version of the paper.

**Acknowledgements** We thank J.F. Kasting for constructive comments on the manuscript. We appreciate proofreading and editing assistance from the GCOE programme. This work was supported by Grants-in-Aid for Scientific Research (KAKENHI) from the Ministry of Education, Culture, Sports, Science and Technology (23103003) and from Japan Society for the Promotion of Science (23340168 and 22740291). This study is a part of the PhD thesis of K.H. submitted to the University of Tokyo.

**Author Contributions** K.H. and Y.A. conceived the initial idea. K.H. constructed the coupled model and performed the calculations. Y.A. contributed to the modelling as well. H.G. provided suggestions on exoplanetary science. All authors discussed the results and implications and commented on the manuscript.

**Author Information** Reprints and permissions information is available at [www.nature.com/reprints](http://www.nature.com/reprints). The authors declare no competing financial interests. Readers are welcome to comment on the online version of the paper. Correspondence and requests for materials should be addressed to K.H. ([keiko@eps.s.u-tokyo.ac.jp](mailto:keiko@eps.s.u-tokyo.ac.jp)).

## METHODS

**Water reservoirs and water budget.** The partitioning of the total water inventory between planetary reservoirs was treated in basically the same way as in ref. 6. Three water reservoirs were considered: atmosphere, magma ocean (a wholly or partly molten region) and solid mantle. The partial pressure of water was calculated at each time step by assuming a solution equilibrium between the atmosphere and the silicate melts at the surface. The water solubility values used were for basaltic melts taken from ref. 31 and were calculated by using the model reported in ref. 27 for a temperature of 2,000 K (see Supplementary Information for the effect of this degassing assumption).

For the incorporation of water into solidifying silicates, two processes were considered: interstitial trapping of water-enriched melts and water partitioning between silicate melts and cumulates. The mass fraction of interstitially trapped melts was assumed to be 1%, as in ref. 6. Although the actual value for a solidifying magma ocean is highly uncertain, a value of 1% is likely to be an overestimate, taking into account the degree of melting estimated for abyssal peridotites when melt separation begins<sup>32</sup>. Few experimental results have been reported on the partition coefficient of water for minerals such as perovskites that make up the deep mantle. We adopted a water partition coefficient of  $10^{-4}$  in our calculations. However, it should be noted that increasing this to  $10^{-2}$  increases the amount of water in the interior at the time of complete solidification by only a factor of 2. This is because interstitial trapping of water-enriched melts dominates.

Because all surface water is in the vapour phase on a solidifying planet, intense hydrodynamic escape of hydrogen is expected to occur during the magma ocean period. We also considered a reduction in the total amount of water due to hydrodynamic escape. The water loss rate was calculated from the energy-limited escape rate for hydrogen<sup>12</sup> by assuming that all of the oxygen produced by dissociation of water vapour would be lost from the atmosphere by oxidation of the magma ocean. Extreme ultraviolet radiation levels for the host star were based on compiled observational data for Sun-like stars, taken from ref. 28, in which the decay with time is expressed as a power-law function of stellar age. A heating efficiency of 0.1 was used throughout all the calculations. Using the higher heating efficiency has less effect on the evolution of type I planets, whereas the solidification time of type II planets becomes shorter in inverse proportion to the heating efficiency (see Supplementary Information).

**Thermal evolution model.** A high degree of melting implies an extremely turbulent magma ocean with a viscosity probably as low as 0.1 Pa (ref. 33). This suggests that the magma ocean is effective in transporting internal heat to the surface. Planetary radiation into space would therefore be the main factor limiting the heat flux from the deep magma ocean. We assumed that the heat flux is given by the difference between the outgoing planetary radiation  $F_{\text{pl}}$  and incoming net stellar radiation  $F_{\text{stl}}$ . On the assumption that the atmosphere has a negligible heat capacity, a thermal evolution model can be formulated on the basis of the heat balance for a planet,

$$C_{\text{p,pl}}(T_{\text{m}}) \frac{dT_{\text{m}}}{dt} = -4\pi R^2 (F_{\text{pl}} - F_{\text{stl}}) \quad (2)$$

where  $C_{\text{p,pl}}(T_{\text{m}})$  is the heat capacity of a planet with an interior potential temperature  $T_{\text{m}}$ , and  $R$  is the planetary radius. Heat flux from the core and heat production by radiogenic elements are neglected. The simple assumption is made that the potential temperature matches the surface temperature  $T_{\text{s}}$ —that is,  $T_{\text{m}} = T_{\text{s}}$ —during the solidification period of the magma ocean. The calculation starts with potential and surface temperatures of 3,000 K, implying a mostly molten mantle, and stops when the solidus temperature at the surface ( $\sim 1,370$  K) is reached.

We calculated the planetary heat capacity, including the latent heat of fusion, as a function of the potential temperature by assuming that the entire silicate portion can transfer heat by convection, and not only the molten part as considered in ref. 6. The heat capacity calculated in this way corresponds to the maximum value, thus providing a conservative estimate of the maximum solidification time for a type I planet. However, both assumptions about the interior temperature profile result in an almost identical solidification time for a type II planet, because the solidification rate is mainly determined not by the heat capacity but by the water loss rate. The adiabatic thermal structure in the interior was calculated according to ref. 29 by using the parameters therein, except for recent experimental data for the solidus and liquidus temperatures at great depth (see Supplementary Information). Differentiation of the mantle and its mineralogy on solidification were not considered in the calculations of the temperature profile, because these would be expected to make a smaller contribution to the overall heat capacity of the planet. See the next section for calculations of planetary radiation and net stellar radiation.

**Atmospheric model.** Planetary radiation was calculated by using a modified version of the radiative–convective equilibrium model in ref. 11, which was originally designed for a steam atmosphere saturated with water vapour and for moderate surface temperatures. However, in the present study the surface temperatures considered are extremely high, exceeding the critical temperature of water. In addition, the relative humidity of the atmosphere can vary because the partial pressure of water is determined by solution equilibrium at the surface. We have extended the grey atmosphere model in ref. 11 to be applicable to the conditions considered herein. The critical point of water was simply treated as the temperature above which no water condensation would occur. For atmospheric layers that were unsaturated by water vapour or for which the temperature was above the critical point, the temperature lapse rate in the troposphere was assumed to be a dry adiabatic temperature gradient, whereas for saturated parcels the lapse rate was assumed to be a pseudo-moist adiabatic temperature gradient, as in ref. 11. The atmosphere is considered to consist of 1 bar of  $\text{N}_2$  in addition to water vapour, the amount of which is determined by the water budget. See Supplementary Information for results calculated with a non-grey atmospheric model in ref. 9, instead of our simple grey model.

For calculations of the net stellar radiation, the solar standard model<sup>30</sup> was adopted to describe the change in stellar luminosity with time. The planetary albedo was fixed at 0.3 in all calculations. The actual value of planetary albedo is highly uncertain, especially because of the unpredictability of cloud coverage with a one-dimensional atmospheric model. In the previous studies (refs 9, 10) a planetary albedo for a thick steam atmosphere was estimated as large as 0.4–0.5, whereas a recent study<sup>34</sup> with a non-grey atmospheric model using the HITEMP database has shown that including weak  $\text{H}_2\text{O}$  lines significantly lowers the planetary albedo.

31. Presnall, D. C. & Hoover, J. D. in *Magmatic Processes: Physicochemical Principles* (ed. Mysen, B. O.) vol. 1, 75–89 (Geochemical Society Special Publication, 1984).
32. Johnson, K. T. M. & Dick, H. J. B. Open system melting and temporal and spatial variation of peridotite and basalt at the Atlantis II fracture zone. *J. Geophys. Res.* **97**, 9219–9241 (1992).
33. Solomatov, V. in *Evolution of the Earth* (ed. Stevenson, D.) 91–119 (Treatise on Geophysics 9, Elsevier, 2007).
34. Kopparapu, R. K. *et al.* Habitable zones around main-sequence stars: new estimates. *Astrophys. J.* **765**, 131, <http://dx.doi.org/10.1088/0004-637X/765/2/131> (2013).

Copyright of Nature is the property of Nature Publishing Group and its content may not be copied or emailed to multiple sites or posted to a listserv without the copyright holder's express written permission. However, users may print, download, or email articles for individual use.